Vector and Tensor Field Topology Simplification on Irregular Grids

Xavier Tricoche, Gerik Scheuermann, Hans Hagen, and Stefan Clauss

University of Kaiserslautern
P.O. Box 3049, D-67653 Kaiserslautern, Germany
E-mail: {tricoche|scheuer|hagen|clauss}@informatik.uni-kl.de

Abstract. Topology-based visualization of planar turbulent flows results in visual clutter due to the presence of numerous features of very small scale. In this paper, we attack this problem with a topology simplification method for vector and tensor fields defined on irregular grids. This is the generalization of previous work dealing with structured grids. The method works for all interpolation schemes.

1 Introduction

Turbulent flows are characterized by the presence of many close vortices of different scales. Such datasets typically result in very complicated pictures when visualized with topology-based methods. This is due to the existence of numerous singularities and corresponding separatrices in the graph depiction: The resulting image is cluttered and the most meaningful features cannot be efficiently extracted. Earlier, we attacked this problem in the case of 2D vector fields defined on a bilinear interpolated curvilinear grid [3]. This method has been extended to second-order symmetric 2D tensor fields over curvilinear grids [6]. In both cases, we achieved a reduction of complicated structures by merging close singularities. The motivation for this operation is the equivalence in the large of several close simple singularities and a single, higher order, singular point.
In the present paper, we use the same basic principle to achieve a topology simplification of planar tensor or vector fields defined on arbitrary grids, with arbitrary interpolation schemes. The major improvement resides in the way of determining the groups of close singularities that are merged: The new method works independently from the underlying cell structure, focusing only on the singularities.
The paper is structured as follows. First, a brief review of existing techniques for simplifying vector fields is given. An overview of the general concepts of vector and tensor field topology is proposed in section 3. Then, we describe the clustering strategy used to partition the field into subdomains where only close singularities are present: This is the purpose of section 4. The fusion of these close singularities is explained in section 5. As last step, the topological structure of these new higher order singularities must be identified: This is done in section 6. Finally, results are shown for an analytic field and a numerical simulation (section 7).

2 Related Work

In [3], we proposed a method for simplifying the topology of planar vector fields defined on curvilinear grids. The grid structure is used to determine cell clusters of close

singularities. This enables local deformations of the grid based upon the piecewise linear nature of the interpolant on the edges.
W. de Leeuw et al. have addressed the issue of vector field topology simplification [4]. Their method simplifies the topological graph by successive removal of connected pairs of critical points. This leads to a significant reduction of the number of critical points and clarifies the topological structure. Yet, no analytic description is provided for the simplified vector field and the method cannot handle arbitrary topological configurations. A cluster based simplification of vector fields has also been presented by B. Heckel et al. [5]. No cell connectivity information is needed and the simplification process reduces substantially the size of large 3D vector data sets. However, possible changes in the vector field topology after simplification can result in structural inconsistency.

3 Vector and Tensor Field Topology

In this section, we briefly review the notion of vector and tensor field topology in the piecewise linear case. Then, we turn to the general case of critical points encountered in continuous piecewise analytic fields.

3.1 Vector Field Topology

The linear topology of planar vector fields is well-known to the visualization community [1]. It consists of critical points (zero locations where streamlines can meet as opposed to any other point) of first order and particular streamlines, called separatrices, that delimit subdomains of the flow where every streamlines are, to some extent, similar. The possible critical points, classified according to the eigenvalues of the Jacobian matrix at their position, are given in Fig. 1. Separatrices are, in this approximation, streamlines that reach or emanate from a saddle point.

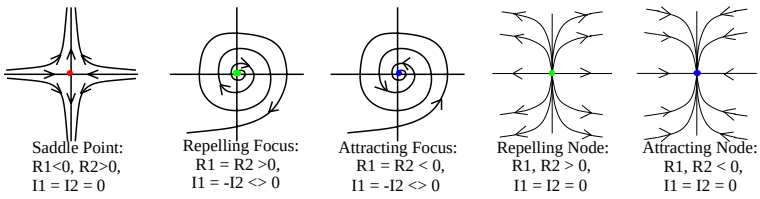

Fig. 1. First order critical points

3.2 Tensor Field Topology

Similar to vector field topology, symmetric second-order 2D tensor field topology has been introduced [2]. Basically, it is defined as the topology of one of the two (bidirectional) eigenvector fields: One defines major (resp. minor) tensor lines as the curves

everywhere tangent to the eigenvector associated with the major (resp. minor) eigenvalue. The singularities are locations where both eigenvalues are equal. These degenerate points appear in two possible types (see Fig. 2). (Note that there exists a wedge point configuration where $S_1 = S_2$.)

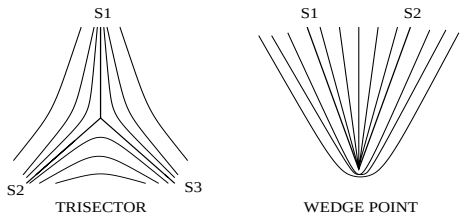

Fig. 2. First order degenerate points

Here, the classification is based upon the so-called δ-invariant: If the symmetric second-order tensor field is denoted by the matrix

$$\begin{pmatrix} T_{11}\, T_{12} \\ T_{12}\, T_{22} \end{pmatrix},$$

we use the linear approximation in the vicinity of a position (x_0, y_0)

$$\begin{cases} \frac{T_{11}-T_{22}}{2} \approx a(x-x_0) + b(y-y_0) + \ldots \\ \quad T_{12} \approx c(x-x_0) + d(y-y_0) + \ldots \end{cases},$$

and define $\delta = ad - bc$.
A trisector point is characterized by a negative value of δ and a wedge point by a positive value. Separatrices are defined as the tensor lines that reach a trisector point along S_1, S_2 or S_3 and a wedge point along S_1 or S_2.

3.3 General Case

In the general case, a singularity (critical or degenerate point) can have one of two types: *center* type (every streamline in the vicinity of the singularity is closed and rotates around without reaching it) or *non-center* type (at least, one streamline reaches the singularity, forming one or more curvilinear sectors). In the non-center case, the characterization is based upon position and type of the curvilinear sectors. These sectors have three possible natures: Hyperbolic, parabolic or elliptic (see Fig. 3). Separatrices are defined as streamlines that bound hyperbolic sectors.

4 Singularity Clustering

Suppose that the singularity positions have been found on an irregular grid. We take them as input for a clustering process that provides us with groups of close singularities. Earlier [3], we proposed a method that preserves the structure of a curvilinear grid. In the present method, we just take the given singularity locations into account.
Let $P_1, \ldots, P_m$ be the positions of the m singularities lying inside a particular cluster. We

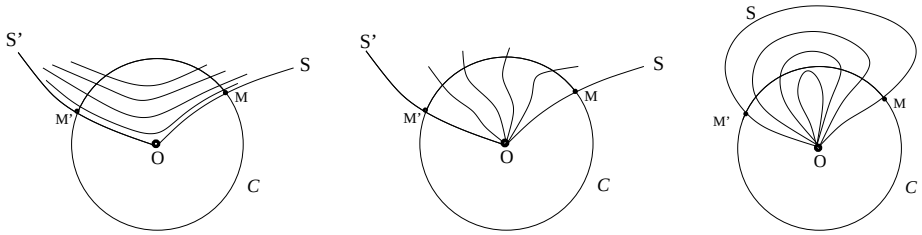

(a) Hyperbolic (b) Parabolic (c) Elliptic

Fig. 3. Sector Natures

want to minimize the approximation error (for a given norm) of these m singularities by a single point, where this point (or cluster *center*) Q is the singularities' mean point (see Fig. 4). The corresponding error is $S = \frac{\sum_{j=1}^{m} \omega_j ||P_j - Q||}{\sum_{j=1}^{m} \omega_j}$, where ω_i is the weight

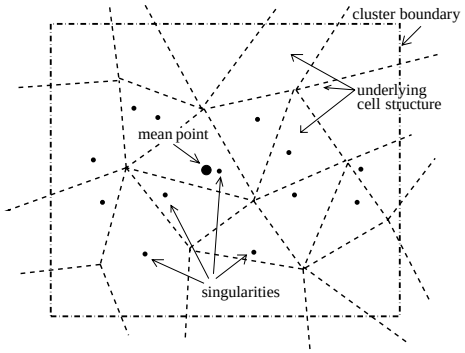

Fig. 4. Cluster singularities and cluster center

associated with the *ith* singularity. (We use here a uniform weighting but one could take into account any measure of singularity strength to determine the weights ω_i.)
The aim of the clustering process is to get a set of clusters that all have an error value smaller than a specified threshold and enclose all singularities.
If a cluster does not satisfy the given error criterion, we split it into sub-clusters. To do this, we introduce the projected variances associated with a given cluster,

$$V_i = \sum_{j=1}^{m} \omega_j (P_j^i - Q^i)$$

where $i \in 0, 1$ is the considered coordinate axis ($P_j = (P_j^0, P_j^1)$).
Now, considering the grid bounding box as initial cluster and putting all cells inside it, the method is as follows.

Step 1. Take as cluster center Q the singularities' mean point.

Step 2. Compute the approximation error S.
If (S > THRESHOLD) go to step 3.
Otherwise stop.

Step 3. Compute the coordinate axis with largest
projected variance (i.e. max(V0, V1)).

Step 4. Split the cluster by a line through Q perpendicular
to the selected coordinate axis, creating 2 sub-clusters.
For each cell contained in the present cluster, check if
it partially lies in each of both sub-clusters (bounding
box intersection test):
Add the indices in the corresponding sub-clusters.
For each sub-cluster, go to step 1.

Remark that the splitting strategy used in the present method is not the only possible one. A cluster can be subdivided in an arbitrary way if the convexity of the sub-clusters is preserved. Nevertheless, our choice leads to clusters with edges parallel to the coordinate axes which enables fast processing.

At the end of this process, we are left with a set of clusters that contain close singularities (according to the metric used) and know what cells are (at least partially) contained in them. The next step is to compute, for each final cluster and for each contained cell, the possible intersections of an edge with the cluster boundary. (This can be done very efficiently because the cluster edges are parallel to the coordinate axes). Adding the 4 cluster corner points to the intersection positions we found, we get a list of positions that we sort next, in a counterclockwise order. Now we isolate the interior domain of the cluster from the rest of the grid. This can be done by removing all cells entirely contained in the cluster (without intersection with cluster boundary) and cutting away the part of every cell intersecting the cluster interior domain: This corresponds to superimposing locally a new small grid on the initial one (see Fig. 5(a)). The cut cells get a modified geometry but keep their interpolation scheme to ensure continuity and consistency with the original field. In particular, the field value along the cluster boundary is unchanged.

5 Singularity Fusion

The technique used is similar to our earlier ideas [3]. We want to get a continuous piecewise analytic field description after modification that ensures the presence of a unique singularity located at the singularities' mean point. Furthermore, we want this description to preserve the field value on the cluster boundary. Consequently, we cover the cluster interior domain as follows: Inserting an additional vertex at the mean point position, we build a triangle star strip connecting this point with every position on the cluster boundary. Furthermore, we associate the new vertex with a singular value. In the vector case, it is a simple zero vector. In the tensor case, every isotropic matrix (of the form $\lambda I_2,\ \lambda \in I\!R$) is a valid choice. Actually, one can show that the isotropic component of a 2D second-order tensor field does not influence the topology of its

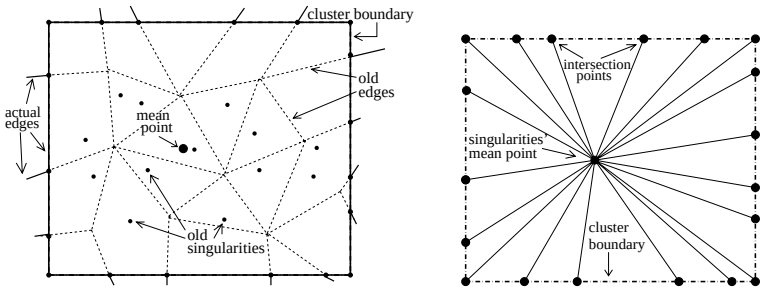

(a) Around a final cluster (b) Inside a final cluster

Fig. 5. New local grid structure

eigenvector fields. For this reason, we take a zero matrix as new artificially created degenerate point (see Fig. 5(b)).

In each of these triangles, we have to define an interpolation scheme that preserves the field value on the cluster boundary. This can be done by using a simple side-vertex interpolation scheme: The position of every point inside such a triangle is determined as shown in Fig. 6, so we get $Q(t) = (1-t)A + tB$ and $P(t,u) = (1-u)\Omega + uQ(t)$. The interpolated value is (with $\boldsymbol{f}$ denoting the considered field)

$$\boldsymbol{f}(P)(t,u) = u\ \boldsymbol{f}(Q(t)), \quad \text{since } \boldsymbol{f}(\Omega) = 0$$

where $\boldsymbol{f}(Q(t))$ is the original value on the cluster boundary. This ensures that the field on the boundary is preserved which guarantees continuity for the new piecewise analytic description. We can also claim that the new artificial singularity is the only one contained in the cluster after modification (otherwise, we would have, for some t, $Q(t) = 0$, and we would have a singular value on the boundary which cannot occur because such a case is rejected during the clustering process).

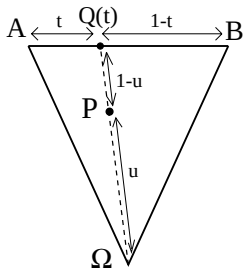

Fig. 6. Side vertex interpolation

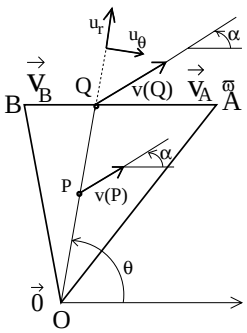

Fig. 7. Vector field in polar coordinates

6 Local Structure Identification

Once such an artificial singularity has been created, its structure must be identified to enable the drawing of the topology. In particular, according to section 3.3, the boundary curves of the hyperbolic sectors must be detected to serve as starting positions for separatrix integration. But first, we need the following property of the side/vertex interpolation scheme: Taking the artificial singularity as polar coordinate origin, the direction of the vector (resp. eigenvector) field does not depend on the radius (see Fig. 7). Practically, it means that separatrices are joining singularity and cluster boundary along straight lines and furthermore, that the search for separatrices positions can be restricted to the cluster boundary. (The proof is straightforward.) In the following, we consider successively vector and tensor cases for the purpose of separatrix position detection.

6.1 Vector Case

We are looking for separatrices that emanate from the singularity along straight lines up to the cluster boundary. In other words, we seek, for each edge on the cluster boundary, positions where the vector field is parallel to the polar coordinate vector $\boldsymbol{u}_r$. At this stage, the positions do not all correspond to an actual separatrix location: They can lie in the middle of a parabolic sector. For this reason, we also detect the positions where the vector field is orthogonal to $\boldsymbol{u}_r$ (that is parallel to $\boldsymbol{u}_\theta$) and check, in the parallel case, the sign of $< \boldsymbol{v}.\boldsymbol{u}_r >$ and, in the orthogonal case, the sign of $< \boldsymbol{v}.\boldsymbol{u}_\theta >$, where $\boldsymbol{v}$ is the vector field value at the considered position. Note that the search for such positions consists of finding the roots of a polynomial equation. The order of this equation depends on the type(s) of interpolation scheme(s) used on the irregular grid. In particular, this order may be different for different edges on the cluster boundary. Typically, if the interpolant is a polynom of degree n, the system to solve will be a polynomial problem of degree $n + 1$. When no algebraic solution can be found, a specific root finder could be applied, based upon the knowledge of the interpolant. Once the interesting positions have been found (marked `PARALLEL+`, `PARALLEL-`, `ORTHOGONAL+` or `ORTHOGONAL-`) and sorted in counterclockwise order along the cluster boundary, we make use of the graphs shown in Fig. 8 to determine the sector types and thus the actual separatrices positions.

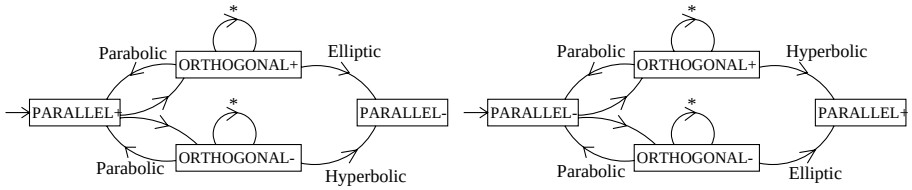

Fig. 8. Sectors discrimination graphs

6.2 Tensor Case

In the tensor case, the principle is basically the same. Nevertheless, because of the sign indeterminacy of the eigenvectors (the eigenvector fields are bidirectional), the sectors discrimination graph cannot be applied (the ORTHOGONAL positions are of no help to distinguish hyperbolic from elliptic sectors). Furthermore, the computation of the eigenvectors induces a higher order of the polynomial equation to solve. Typically, if the tensor field interpolant has order n, then the determination of the PARALLEL positions leads to a polynomial equation of order $n + 2$. After that, we sort the PARALLEL positions in counterclockwise order and look at the angle variation of the eigenvector field between two consecutive PARALLEL positions as follows. Depending on the sector type, one gets

- $\Delta\alpha = \theta$ in the *parabolic* case
- $\Delta\alpha = \theta - \pi$ in the *hyperbolic* case
- $\Delta\alpha = \theta + \pi$ in the *elliptic* case

which enables a sector type identification (see Fig. 9).

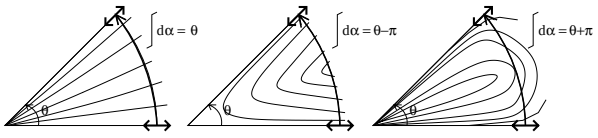

Fig. 9. Angle variation in the parabolic, hyperbolic and elliptic case

7 Results

We present here the results of our method applied to an artificial turbulent vector field and to a tensor field provided by a numerical simulation.
The first dataset is a 2D vector field defined on the Delaunay triangulation of an unstructured point set. The interpolation scheme is piecewise linear. The grid has 400 vertices, ranging from -5 to +5 in x and y. The original topology contains 189 critical points and 380 separatrices (see Fig. 10). We first simplify this complicated topology with a clustering threshold of 0.5. The graph has now 114 critical points and 286 separatrices (see Fig. 12(a)). To ease the interpretation, higher order singularities are depicted as big circles. Using a threshold of 1.5, there are 81 critical points and 188 separatrices remaining (Fig. 12(b)). Note that the simplification process does not affect the topology close to the grid boundary (which explains the presence of many singularities) to preserve consistency to the original data.
The second dataset is a numerical simulation of a turbulent flow: Fig. 11 shows the topology of the rate of strain tensor field of a swirling jet. The vertices lie on a structured point set (101 x 124) that we triangulate first. The grid ranges from -3.85 to 3.85 in x and 0 to 9.87 in y. The original topology is characterized by 67 degenerate points and 144 separatrices. We start simplifying with a threshold of 0.5: We get 34 degenerate points and 78 separatrices. Once again, the clusters are shown (Fig. 13(a)). If we move to a larger value for the clustering threshold (1.0), the topology simplifies dramatically as shown in Fig. 13(b): 18 degenerate points are present and only 42 separatrices remain.

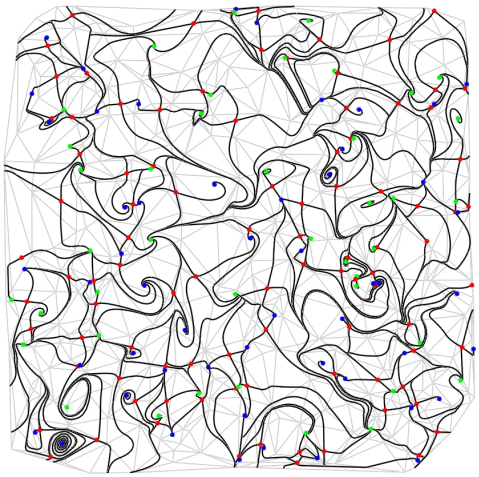

Fig. 10. 1st example: Vector case

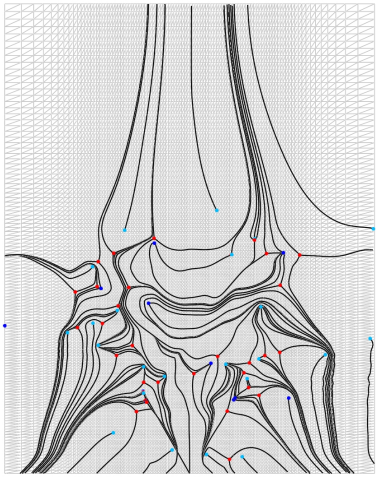

Fig. 11. 2nd example: Tensor case

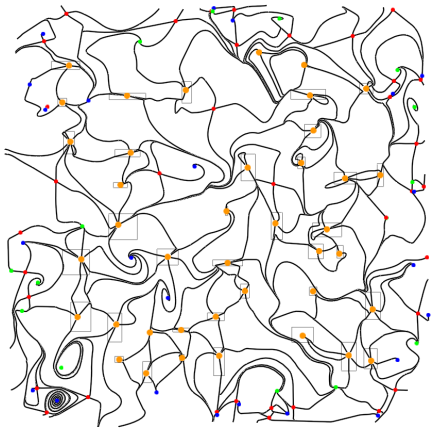

(a) threshold = 0.5

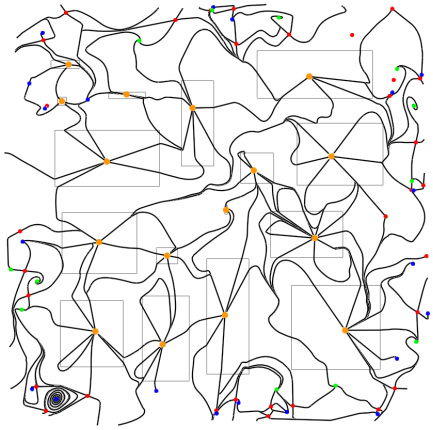

(b) threshold = 1.5

Fig. 12. 1st example: Simplified topologies

8 Conclusion

We have presented a method for simplifying the topology of vector and tensor fields defined over irregular grids with arbitrary interpolation schemes. Our technique is based upon a clustering strategy that handles the singularities (critical or degenerate points), omitting the underlying cell structure. It permits a flexible local topology simplification by merging the close singularities lying in the same final cluster while providing piecewise analytic description for the field after simplification. The method produces clarified depictions and preserves topological consistency with the original data.

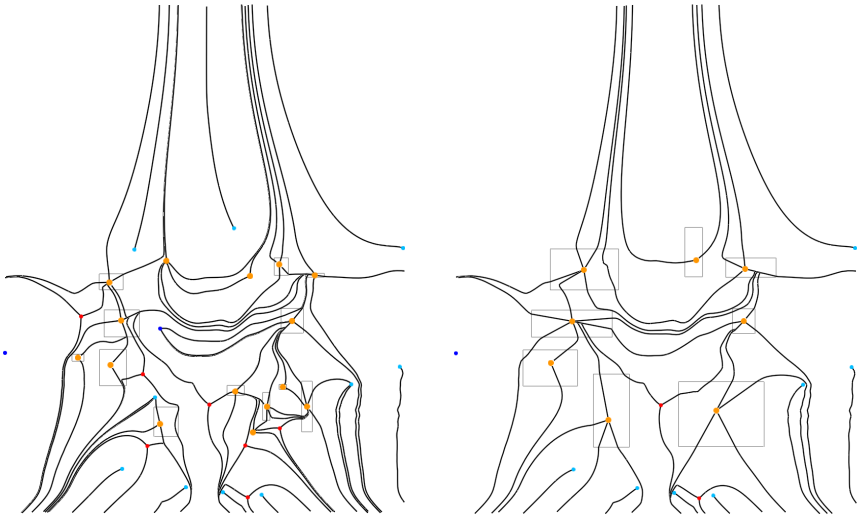

(a) threshold = 0.5 (b) threshold = 1.0

Fig. 13. 2nd example: Simplified topologies

Acknowledgment

The authors wish to thank Wolfgang Kollmann, MAE Department of the University of California at Davis, for providing the swirling jet dataset.

References

[1] Helman J.L., Hesselink L., *Visualizing Vector Field Topology in Fluid Flows*. IEEE Computer Graphics and Applications, 1991, pp.36-46.

[2] Delmarcelle T., *The Visualization of Second-Order Tensor Fields.* PhD Thesis, Stanford University, 1994.

[3] X. Tricoche, G. Scheuermann, H. Hagen, *A Topology Simplification Method for 2D Vector Fields.* In Proceedings IEEE Visualization'00, IEEE Computer Society, Los Alamitos CA, 2000, pp.359-366.

[4] de Leeuw W., van Liere R., *Collapsing Flow Topology Using Area Metrics*. In Proceedings of IEEE Visualization '99, IEEE Computer Society, Los Alamitos CA, 1999, pp.349-354

[5] Heckel B., Weber G., Hamann B., Joy K.I., *Construction of Vector Field Hierarchies*. In Proceedings of IEEE Visualization '99, IEEE Computer Society, Los Alamitos CA, 1999, pp.19-25.

[6] Tricoche X., Scheuermann G., Hagen H., Clauss S., *Scaling the Topology of Symmetric Second-Order Tensor Fields* In NSF/DoE Lake Tahoe Workshop on Hierarchical Methods for Scientific Visualization, October 2000.